Spin observables for the $pd \leftrightarrow \pi^+ t$ reaction around the Δ resonance

L. Canton, G. Cattapan, and G. Pisent
Istituto Nazionale di Fisica Nucleare, Sezione di Padova, and Dipartimento di Fisica, Università di Padova, Via F. Marzolo 8, I-35131 Padova, Italy

W. Schadow
Department of Physics and Astronomy, Ohio University, Athens, Ohio 45701

J. P. Svenne
Physics Department, University of Manitoba, and Winnipeg Institute for Theoretical Physics, Winnipeg, Manitoba, Canada R3T 2N2

(Received 5 December 1997)

The proton analyzing power A_{y0} and the deuteron tensor analyzing power T_{20} are evaluated for the $pd \leftrightarrow \pi^+ t$ process, in the energy region around and above the Δ resonance. These calculations extend a previous analysis of the excitation function and differential cross section, based on a model embodying one- and two-body p-wave absorption mechanisms and isobar excitation. The three-nucleon bound state and the pd scattering state are evaluated through Faddeev techniques for both the Bonn and Paris potentials. The spin variables exhibit a greater sensitivity to the number of included three-nucleon partial waves than the cross sections, while the role played by the initial- or final-state interactions appears to be small. The results for the tensor analyzing power at backward angles show a non-negligible dependence on the potentials employed, consistently with what has been previously found for the cross sections. The calculation of spin observables gives a clear indication that other reaction mechanisms (presumably s-wave two-body absorption) have to be included in the model, in order to reproduce the experimental data below the Δ resonance, in analogy with the simpler $pp \leftrightarrow \pi d$ process. [S0556-2813(98)03004-0]

PACS number(s): 25.80.Ls, 25.40.Qa, 25.10.+s, 13.75.Cs

I. INTRODUCTION

Pion absorption/emission processes on $A=3$ nuclei offer a unique possibility for testing our present understanding of pion-baryon interactions and reaction mechanisms with a minimum of *ad hoc* phenomenological assumptions. It is now possible, in fact, to give a microscopic description of both the nuclear bound state and the three-nucleon dynamics in the incoming (or exit) channel through modern few-body techniques.

A first step towards this goal has been accomplished in a recent paper [1], where pion emission/absorption reactions on tritium have been studied in the energy region around the Δ resonance. The elementary emission/absorption processes are given by the direct, one-nucleon mechanism, and by the two-body mechanism, proceeding through Δ excitation. The former is described by a nonrelativistic πNN vertex, the latter by a $\pi N\Delta$ vertex, followed (or preceded) by isobar propagation, and a $\Delta N \leftrightarrow NN$ transition mediated by π and ρ exchange. The three-nucleon bound and scattering states in the initial and final channels have been evaluated through numerical solution of the Alt-Grassberger-Sandhas (AGS) [2] equations for realistic NN potentials, by resorting to the Ernst-Shakin-Thaler (EST) expansion method [3,4], to produce a finite-rank representation of the NN interactions. With this representation, the π-production amplitude including the three-nucleon correlations can be obtained by solving an integral equation where the off-shell extension of the plane-wave amplitude represents the driving term. This approach is similar to a recent treatment of tritium photodisintegration [5]. The transition amplitudes have to be decomposed into three-nucleon partial waves, whereas the pion-tritium motion is represented by a three-dimensional plane-wave state. The calculation has been performed in momentum space, and details about the partial-wave formalism can be found elsewhere [1,6].

The phenomenological parameters entering the above calculations are essentially the coupling strengths and cutoffs at the meson-baryon vertices. These parameters had been tuned previously through the analysis of the simpler $\pi d \leftrightarrow pp$ reaction [7,8], over a large experimental database, including cross sections and polarization observables. Hence, the analysis of Ref. [1] can be regarded as a parameter-free calculation, aiming at ascertaining to what extent the assumed model of the pion-nucleus dynamics can be extended from the two-nucleon to the three-nucleon system. These calculations have been compared with experimental integral and differential cross sections. The role played by the final- or initial-state interactions (FSI/ISI) has been studied, and the convergence with respect to the number of included partial-wave three-nucleon states has been tested. It turned out [1] that the inclusion of higher partial waves and nuclear correlations have a comparable effect on the cross sections. Good results could be obtained in the considered energy region with both Bonn [9] and Paris [10] potentials, the latter producing a lower excitation function with respect to the Bonn B potential, and slightly better results for the differential cross sections at backward angles and high energies. Around the resonance, and for not too large angles, however, the results for the two potentials differ only in the normalization of the cross sections, with the excitation function for the

Paris potential being about 25% lower than the Bonn B result.

In the present paper we extend the analysis to spin observables (such as the asymmetry A_{y0}, and the deuteron tensor analyzing power T_{20}), and to a larger energy region, in order to get a deeper insight into the merits and limitations of the model employed for the π-three-nucleon dynamics.

For the $\pi d \leftrightarrow pp$ reaction, the polarization observables are known to be much more sensitive to the details of the dynamical model than the unpolarized cross sections [7,8,11]. For this reason, the large variety of spin data has never been reproduced with complete success, in spite of the increasing complexity of the theoretical models. In particular, the proton analyzing power A_{y0} is one of the most difficult observables to reproduce since it depends on both the magnitude and the relative phases of the intervening helicity amplitudes. A similar situation appears here for the $\vec{p}+d \rightarrow \pi^+ + t$ reaction. We investigated how much this observable is affected by the partial-wave truncation, and by the inclusion of nuclear correlations in the initial channel. We found a more pronounced sensitivity to the number of included three-nucleon partial-wave states, with respect to the cross sections. When the representation is enlarged to include 18 two-body partial-wave states and S, P, and D orbital states in the intermediate Δ propagation, the theoretical results move towards the experimental points. The effects of the three-nucleon correlations in the initial state, on the other hand, turn out to be less important. As for T_{20}, one can obtain the general trend of the experimental data around the resonance, the results exhibiting a moderate sensitivity to the chosen NN potential at forward angles, and a greater sensitivity at large angles, consistently with the analysis of the unpolarized cross sections.

This model, in its present form, has been built for an analysis around the resonance region, where the intermediate ΔN dynamics has to be treated explicitily. As is well known, a theoretical evaluation of the Δ width in the nuclear environment is still beyond present possibilities, since it would entail a consistent solution of the coupled $\pi NNN - \Delta NN - NNN$ problem. Lacking this theoretical ingredient, we choose to parametrize the resonance width phenomenologically, starting from the experimental cross section for the $\pi d \rightarrow pp$ reaction. This phenomenological parametrization implicitly takes into account the nonperturbative aspects of the intermediate Δ propagation within the two baryon subsystem; it proved successful both in the description of the $\pi d \leftrightarrow pp$ data from threshold [12] up to the resonance region [7,8], and in the three-nucleon calculations of Ref. [1]. Here, we extend the analysis of $pd \leftrightarrow \pi t$ processes beyond the resonance region for both the cross sections and spin observables, and compare the outcome of this effective parametrization with the standard relativistic treatment of the Δ width, which applies to a free Δ [13,14]. One finds that the former parametrization provides better differential cross section in the resonance region, whereas the alternative description works better with increasing energy. This suggests that nonperturbative effects in the off-shell Δ propagation are non-negligible in the resonance region, while their importance decreases at higher energies.

The data are not well reproduced in the low-energy region. This is particularly true for the tensor analyzing power at forward angles, where one fails even in reproducing the trend of the experimental points. This had to be expected, because in the present calculations only p-wave absorption mechanisms are considered. At low energies, one expects non-negligible contributions from s-wave pion absorption, involving π rescattering on a second nucleon. Such mechanisms play an important role in the π-absorption process, and have to be taken into account in extending the present analysis from the high-energy to the low-energy region, as has been shown in Ref. [12] for the simpler $pp \leftrightarrow \pi^+ d$ reaction.

The formalism relating cross sections and polarization observables to the transition amplitudes as given in the present approach is reviewed in Sec. II. The results of calculations are shown and discussed in Sec. III. Finally, Sec. IV contains the summary and conclusions.

II. THEORY

The amplitude for the $pd \leftrightarrow \pi^+ t$ process can be written in terms of the matrix element

$$A^{\rm tot} = {}^{(-)}_{\mathcal{S}}\langle \mathbf{q}, \psi_d | \mathcal{A} | \psi_{\rm BS} \rangle_{\mathcal{S}} | \mathbf{P}_0^{\pi} \rangle . \tag{1}$$

The states $|\psi_{\rm BS}\rangle_{\mathcal{S}}$ and ${}^{(-)}_{\mathcal{S}}\langle \mathbf{q}, \psi_d|$ describe the final three-nucleon bound state (BS) and the initial three-body scattering state, respectively, and are assumed to be properly antisymmetrized. For both bound state and scattering regimes, we use herein the same three-nucleon states previously employed in Ref. [1]. Henceforth, we refer to that paper for any details about the Faddeev-based calculation of the three-nucleon states. The states $\langle \mathbf{q}|$ and $|\mathbf{P}_0^{\pi}\rangle$ are the plane-wave states for the two fragments in the asymptotic channels. The momenta P_0^{π} and q are the on-shell momenta in the c.m. frame for the (outgoing) pion and (incoming) nucleon, respectively.

In the operator $\mathcal{A}$ we specify the reaction mechanisms under consideration. To avoid double countings, purely nucleonic intermediate states must be avoided in $\mathcal{A}$, since the intermediate propagation of three nucleons is taken into account to all orders when calculating the three-nucleon dynamics in the final state. These amplitudes are decomposed in three-nucleon partial waves, while the pion-nucleus wave is kept three-dimensional. We omit the details on the representation employed since all this has been thoroughly discussed in previous papers [1,6]. Herein, we limit ourselves to mention that the three-body states are defined in momentum space and the partial-wave decomposition is discussed within the jI coupling scheme. The index α collectively denotes the whole set of quantum numbers, namely spin, total angular momentum, and isospin of the pair (s, j, and t, respectively) orbital, spin, total angular momentum, and isospin for the spectator (λ, σ, I, and τ) and finally the three-nucleon total angular momentum, isospin and associated third components, JJ^z and TT^z. To calculate spin observables we adopt the helicity formalisms as introduced by Jacob and Wick [15]. The phase conventions, however, are those defined in Ref. [16]. We transform the jI coupling scheme of our amplitudes into a channel–spin representation, where the angular momentum of the spectator particle, λ, is coupled to channel spin K (which is the coupling of the spectator-

nucleon spin, σ_1, to the deuteron spin, j) to give the total angular momentum J. The transformation is

$$|(\lambda(\sigma_1 j)K)J\rangle = \sum_I (-)^{\sigma_1+\lambda+I}\hat{K}\hat{I}\begin{Bmatrix} j & \sigma_1 & K \\ \lambda & J & I \end{Bmatrix}|(j(\lambda\sigma_1)I)J\rangle. \tag{2}$$

The amplitude in this new λ-K representation will be compactly indicated as

$$A((\lambda,K)J,\mu_b)\equiv\sqrt{\frac{4\pi}{2J+1}}(-)^{1/2-J^z}A(q,(\lambda K)J,-J^z,E). \tag{3}$$

We observe that in this representation the pion and nucleon relative states of motion are treated differently, and, for convenience, we prefer to discuss the amplitudes in terms of the (inverse) pion absorption process. By doing so, the initial state is *not* decomposed into partial waves, while the final state is. The quantization axis is parallel to P_0^π, thus it is the helicity axis for the incoming pion (obviously, the helicity of the pion μ_a is zero). For the target particle, the triton, we take the same axis, but pointing in the opposite direction. Hence, for the target particle, we have to rotate the frame of 180° around the normal to the scattering plane. Because of this rotation the target helicity is $\mu_b=-J^z$, and the phase factor appears in the equation above. We construct the partial-wave helicity amplitude

$$f^{/\,\mu_b}_{\mu_c\mu_d}(J)=\sum_{\lambda,K}\langle\mu_c\mu_d J|\lambda K J\rangle A((\lambda K)J,\mu_b), \tag{4}$$

where μ_c is the helicity of the outgoing nucleon, and μ_d is the helicity of the deuteron. Given that μ_a is zero, we use the symbol ''/'' in place. The coefficients $\langle\mu_c\mu_d J|\lambda K J\rangle$ provide the Jacob-Wick transformation from the channel spin to the helicity representation with the phase conventions adopted in Ref. [16]

$$\langle\mu_c\mu_d J|\lambda K J\rangle = (-)^{K-s_d+\mu_c}C(s_c,s_d,K;\mu_c,-\mu_d,\mu_c-\mu_d) \times C(K,J,\lambda;\mu_d-\mu_c,\mu_c-\mu_d,0), \tag{5}$$

where C are the usual Clebsh-Gordan coefficients in the notation of Ref. [6].

The expansion in terms of reduced rotation matrices yields the angular dependent helicity amplitudes

$$F^{/\,\mu_b}_{\mu_c\mu_d}(\theta)=\sum_J\frac{2J+1}{4\pi}f^{/\,\mu_b}_{\mu_c\mu_d}(J)d^J_{(-\mu_b)(\mu_c-\mu_d)}(\theta), \tag{6}$$

where θ is the scattering c.m. angle for the outgoing nucleon. Of the twelve helicity amplitudes, symmetry principles lead to 6 independent ones (we omit the angular dependence for brevity). Thus

$$\begin{aligned} F^{/\,1/2}_{1/2\,1}&=-F^{/\,-1/2}_{-1/2\,-1},\\ F^{/\,1/2}_{1/2\,0}&=F^{/\,-1/2}_{-1/2\,0},\\ F^{/\,1/2}_{1/2\,-1}&=-F^{/\,-1/2}_{-1/2\,1},\\ F^{/\,1/2}_{-1/2\,0}&=-F^{/\,-1/2}_{1/2\,0},\\ F^{/\,1/2}_{-1/2\,1}&=F^{/\,-1/2}_{1/2\,-1},\\ F^{/\,1/2}_{-1/2\,-1}&=F^{/\,-1/2}_{1/2\,1}. \end{aligned} \tag{7}$$

Finally, we obtain the helicity amplitudes for the π production process from time-reversal symmetry. Accordingly, the time-reversal amplitudes are related by the equations

$$F^{\mu_c\mu_d}_{/\,\mu_b}(\theta)=(-)^{\mu_c-\mu_d+\mu_b}\frac{|p_a|}{|p_c|}F^{/\,\mu_b}_{\mu_c\mu_d}(\theta), \tag{8}$$

where on the left-hand side θ is the scattering angle for the produced pion, while on the right-hand side it refers to the angle for the outgoing nucleon. Also, p_a is in our case P_0^π, while p_c is q. By means of these relations, we define

$$\begin{aligned} Z_1(\theta)&=F^{/\,1/2}_{1/2\,1},\\ Z_2(\theta)&=-F^{/\,1/2}_{1/2\,0},\\ Z_3(\theta)&=F^{/\,1/2}_{1/2\,-1},\\ Z_4(\theta)&=F^{/\,1/2}_{-1/2\,0},\\ Z_5(\theta)&=-F^{/\,1/2}_{-1/2\,1},\\ Z_6(\theta)&=-F^{/\,1/2}_{-1/2\,-1}, \end{aligned} \tag{9}$$

having factored out the momentum ratio since it is taken into account at a later stage. Well-known spherical tensor algebra [16] leads to the following expression:

$$A_{y0}=-4\frac{\mathrm{Im}(Z_1Z_5^*+Z_2Z_4^*+Z_3Z_6^*)}{I_0} \tag{10}$$

for the analyzing power for the reaction $\vec{p}+d\rightarrow\pi^++t$. The quantity I_0 is defined as

$$I_0=2(|Z_1|^2+|Z_2|^2+|Z_3|^2+|Z_4|^2+|Z_5|^2+|Z_6|^2) \tag{11}$$

and gives the differential cross section

$$\frac{d\sigma}{d\Omega}(\theta)=\frac{c}{2}I_0 \tag{12}$$

for the pion absorption reaction, or

$$\frac{d\sigma}{d\Omega}(\theta)=\frac{c}{6}\left(\frac{P_\pi^0}{q}\right)^2 I_0 \tag{13}$$

for the inverse reaction. The constant c corresponds to the phase-space factor

$$c=(2\pi)^4\frac{q}{P_\pi^0}\frac{E_\pi E_t E_N E_d}{(E^{\mathrm{tot}})^2}, \tag{14}$$

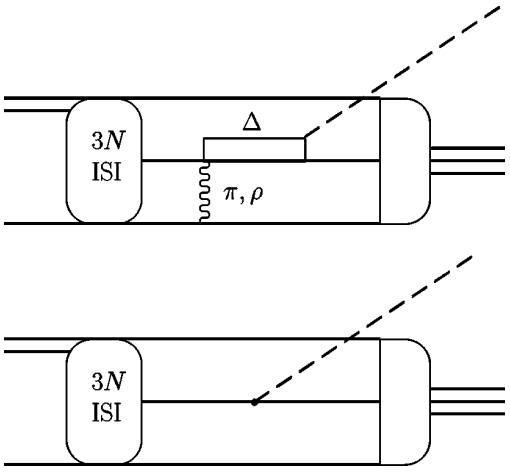

FIG. 1. Diagrams included in the present analysis. On top, the Δ-rescattering mechanism is composed of the $\pi N\Delta$ vertex, the Δ intermediate propagation, and the ΔN transition via π and ρ exchange. On bottom, the direct πNN mechanism is shown. For both mechanisms, the three-nucleon correlations in the initial state are represented by the oval on the left, while on the right the three-nucleon bound state is denoted by the half oval.

with the relativistic energy of the fragments given by

$$E_\pi = \sqrt{m_\pi^2 + P_0^{\pi 2}},$$
$$E_t = \sqrt{M_T^2 + P_0^{\pi 2}},$$
$$E_N = \sqrt{M^2 + q^2}, \tag{15}$$
$$E_d = \sqrt{M_D^2 + q^2},$$
$$E^{\rm tot} = E_N + E_d = E_\pi + E_t .$$

Here, M_D, M_T, are the deuteron and tritium masses, respectively.

From the same helicity amplitudes, we have calculated also the deuteron tensor analyzing power T_{20}

$$T_{20} = \sqrt{2}\frac{(|Z_1|^2 - 2|Z_2|^2 + |Z_3|^2 - 2|Z_4|^2 + |Z_5|^2 + |Z_6|^2)}{I_0}. \tag{16}$$

III. RESULTS

In a previous article [1], it has been shown that the energy dependence and angular distribution of the $pd \leftrightarrow \pi^+ t$ reaction cross section around the Δ resonance could be reproduced reasonably well with a meson-exchange isobar model with the π-nucleon interaction mediated by the p-wave πNN and $\pi N\Delta$ vertices. The pion production/absorption diagrams included in that model are shown in Fig. 1.

In the same paper, the normalization of the cross section was found to be quite sensitive to the NN potential model employed (Paris, Bonn A, or Bonn B), while the angular distributions were found to be less sensitive, with the exclusion of the region at backward angles, where a non-negligible dependence upon the nuclear potential has been shown. At the resonance peak, the three-body dynamics in the nucleon-deuteron channel (ISI) have been calculated via a Faddeev-AGS computational scheme, and the effect of the inclusion of a higher number of three-nucleon partial waves has been also analyzed. In comparing the results, it turned out that these two aspects were comparable in that they both affected the unpolarized cross section by roughly the same amount. Indeed, the Faddeev-AGS calculation of the three-nucleon dynamics in the initial state gave a 4% effect in the cross section, and a comparable 4% effect was found in passing from a calculation including 82 three-nucleon partial waves, to our largest calculation with 464 partial waves.

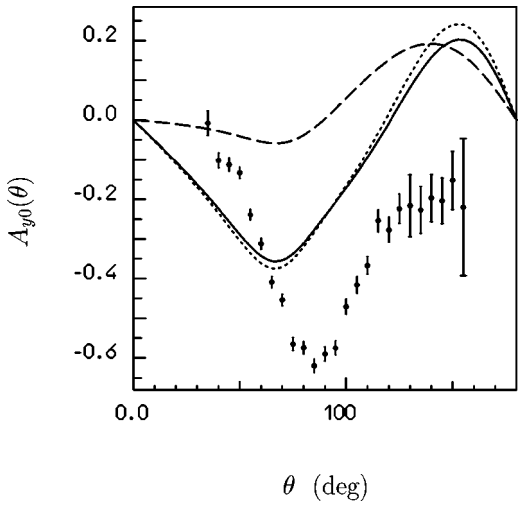

FIG. 2. Analyzing power A_{y0} of the reaction $\vec{p} + d \rightarrow \pi^+ + t$ for incident protons at 350 MeV . The dashed line includes only intermediate ΔN S states, while the remaining two curves include S, P, and D intermediate ΔN states and 464 three-nucleon partial waves. The dotted line contains the contribution of ISI, while the full line does not. All the results have been obtained with the Bonn B potential.

We refer to the article [1] for all the details about the model, and for the list of partial waves included in the various calculations. Herein, we limit ourselves to stress that the main difference between the 82- and 464-state calculations is due to the inclusion in the latter of S, P, and D waves for the intermediate ΔN subsystem, while in the former case only S waves were retained.

In this section, we use the same amplitudes which have been calculated previously in Ref. [1] and take the analysis one step further by calculating the polarization observables according to the methods described in the previous section. The results for the proton analyzing power A_{y0} are compared in Fig. 2 with the data obtained in Ref. [17] for the isospin-related reaction $\vec{p} + d \leftrightarrow \pi^0 + {}^3{\rm He}$ at 350 MeV. Assuming charge independence, the results have to be equal. The dashed line in the figure exhibits the result of the calculation including 82 three-nucleon intermediate partial waves, and only S states for the intermediate ΔN system. In this case, the results are very different from the trend of the experimental data; however, the dashed curve is comparable in shape and magnitude with previous theoretical results shown in Ref. [18].

The other two curves exhibit the results of the calculations including 464 $3N$ states and differ between each other by the fact that the dotted line includes the effects of the three-nucleon dynamics in the initial state, while the full line

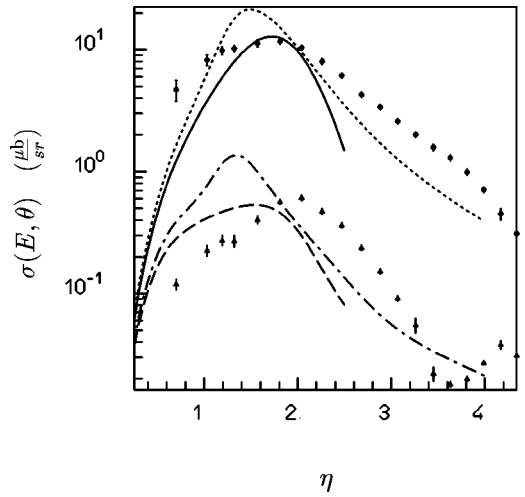

FIG. 3. Differential cross section at 0° and 180° versus the parameter η calculated with the Bonn B potential. The full (dashed) line represents the forward (backward) cross section calculated with the isobar width parametrized starting from the πd absorption cross section, while for the dotted (dotted-dashed) curves the free isobar width has been employed.

does not. In both cases the intermediate ΔN states have been included up to D waves. In comparing the two curves, it is clear that the consequences for A_{y0} due to the three-nucleon dynamics in the initial state are not very large. Instead, the difference with the dashed curve is a clear indication that the polarization observables are much more sensitive to the inclusion of a large, possibly converged, set of states than what happens for the unpolarized observables. In particular, an important aspect which cannot be neglected is played by the P and, to a lesser extent, by the D orbital states of the ΔN subsystem. It was also found that orbital states higher than D waves give virtually no further change for this observable, at least at the resonance energy.

In Fig. 3 the differential cross section at forward and backward angles is shown as a function of the parameter η, defined as the pion-nucleus c.m. momentum, in units of pion masses (times c). The experimental data have been obtained at Saclay [19] for the π^0 production reaction. The full circles represent cross section data at forward angles, and the triangles are the corresponding data at backward angles. The experimental results are compared with the theoretical calculation assuming charge independence (implying a factor 2 between π^+ and π^0 production). The full (dashed) line exhibits the calculation at forward (backward) angles performed with the model introduced in Ref. [1], and correspond to results obtained under the same circumstances as the results for A_{y0} shown by the full line in Fig. 2.

These calculations have been tailored for the reproduction of the pion production reaction in a region limited around the Δ resonance. Indeed, the main limitation in the energy range derives from the treatment of the width of the Δ resonance, whose range of validity is restricted in the region below $\simeq 2.5$ for η. The explicit parametric form of the isobar width Γ_Δ is given in Ref. [7]; it has been derived starting from the shape of the experimental π-absorption cross section on deuterons, $\sigma(E)$, by imposing the condition

$$\sigma(E)=\frac{D}{(E-E_r)^2+\dfrac{\Gamma_\Delta(E)^2}{4}}, \tag{17}$$

plus the additional condition that at the resonance peak E_r, the isobar width coincides with the experimental value of 115 MeV (this last condition fixes also the constant D).

The same energy dependence has been employed without further changes in previous analyses for the $\pi^+ d \leftrightarrow pp$ (Ref. [8]) and $pd \rightarrow \pi t$ (Ref. [1]) reactions. In this paper, as previously done in Ref. [1], we have used the same parameters (i.e., coupling constants and cutoffs) defined in Ref. [8], without further modifications. However, in the analysis herein we extended the energy range above the Δ resonance by going up to $\eta \simeq 4$. In order to accomplish this, we considered a different parametrization of the isobar width,

$$\Gamma_\Delta=\frac{2}{3}\frac{f^2_{\pi N\Delta}}{4\pi}\frac{q^3}{m^2_\pi}\frac{M}{\sqrt{s}}, \tag{18}$$

where q is the pion momentum in the c.m. frame, $\sqrt{s}$ is the invariant πN mass, M and m_π are the nucleon and pion masses, respectively, and $f_{\pi N\Delta}$ is the coupling constant of the $\pi N\Delta$ vertex.

This simple parametrization is commonly used in the analysis of the πN scattering processes [13,14] and therefore refers to the width of a *free* Δ. It has the advantage of not being restricted to a limited energy range, and hence can be employed in the region well above the resonance peak where the previous parametrization [Eq. (17)] breaks down. A comparison between the energy dependence of the two widths has been done in Ref. [7].

The dotted (dashed-dotted) line in Fig. 3 shows the forward (backward) cross section results calculated with the isobar width expression given by Eq. (18). These results are spanning a wider energy region above the isobar resonance, and they improve the description of the reaction in the higher energy range, starting already from $\eta \geqslant 2$. In contrast, the results in the lower energy region are best reproduced by the previous set of calculations which employs the parametrization given by Eq. (17). At the present stage, there is no definitive explanation for this behavior. We may however argue that, as the pion momentum η increases to a value around 2, the isobar in the intermediate ΔNN propagation tends to behave as a free-particle propagation, while at lower energy the importance of the ΔN higher order interactions prevents a description in terms of free isobar propagation. If this is the case, the superior results obtained at lower energy by the parametrization from Eq. (17) can be understood in the light of the fact that the Δ width obtained directly from the experimental $\pi d \rightarrow pp$ excitation function must include, albeit in some phenomenological and approximate way, the ΔN higher order interactions, while the baryon-baryon interactions are certainly excluded when the width is parametrized from the πN scattering data.

Figure 4 differs from the previous one in that the Paris NN potential has been employed instead of the Bonn B one. Except for this change, for the four curves the same symbolism of Fig. 3 has been adopted. The forward peaked differential cross sections are very similar for the two potentials,

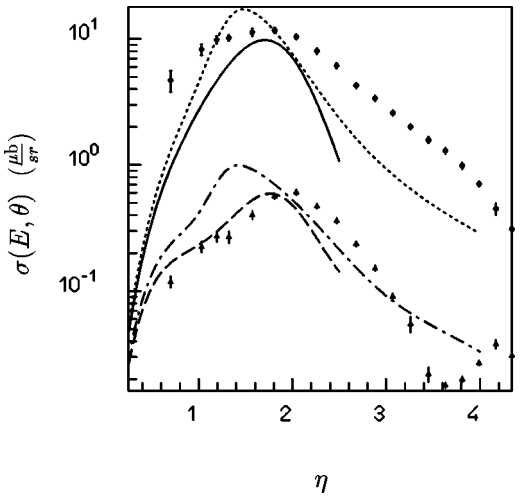

FIG. 4. Same results as in the previous figure but with the Paris potential.

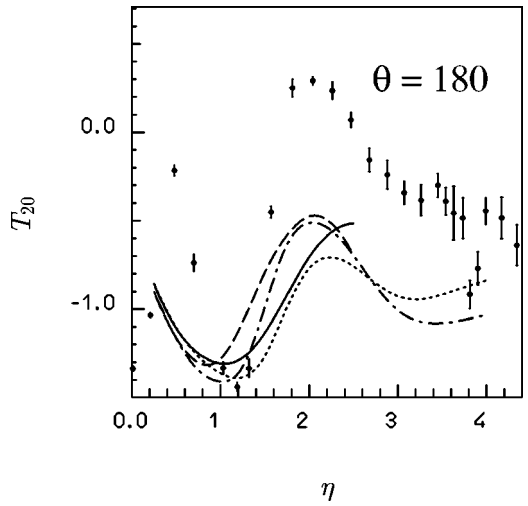

FIG. 6. Same observable as in the previous figure but for backward direction. The curves are defined with the same symbolism.

the only difference being in the normalization of the corresponding curves. As already discussed in Ref. [1], the results with the Paris potential are about 25% smaller than the results obtained with the Bonn *B* potential. The results at backward angles show a greater sensitivity to the *NN* interaction, since the differences in this case cannot be attributed to a simple change in the normalization of the results. At lower energy, the results at backward angles obtained with the Paris potential reproduce better the trend of the experimental data. At higher energy, the calculations at backward angles for both potentials fail to reproduce the dip around $\eta \simeq 3.6$. In a previous study [20], the presence of this ''bump'' in the backward-angle data has been explained in terms of possible three-body pion production mechanisms. Such mechanisms are not contemplated in the present analysis.

In Fig. 5, the results for the deuteron tensor analyzing power T_{20} at forward angles are shown. The experimental results are those reported in Ref. [19]. The full and dotted lines represent the results obtained with the Bonn potential, while the dashed and dashed-dotted curves are similar calculations with the Paris potential. Furthermore, the solid and dashed lines correspond to the isobar width parametrized according to Eq. (17), while for the dotted and dashed-dotted lines Eq. (18) has been used. Independently of the isobar width and/or the nuclear potential employed the differences are not very large. The results at lower energy are very different from the experimental data while at higher energy [for $\eta \geqslant 2$, where mainly Eq. (18) can be used] the reproduction is much better. A possible explanation for this behavior can be attributed to some low-energy production mechanisms still missing in the present analysis. A natural candidate is the mechanism triggered by the πN interaction in *S* wave. It is well known that this mechanism is quite relevant in the $\pi d \leftrightarrow pp$ reaction around the resonance [1,7,8] and of fundamental importance for the description of the same reaction at threshold. It is possible, and indeed very likely, that the same mechanism becomes more and more important at lower energies also for the $pd \leftrightarrow \pi^+ t$ process. The discrepancies seen at lower energies not only in Fig. 5, but also in the forward-peaked differential cross section (Figs. 3 and 4), could be possibly explained by such mechanisms.

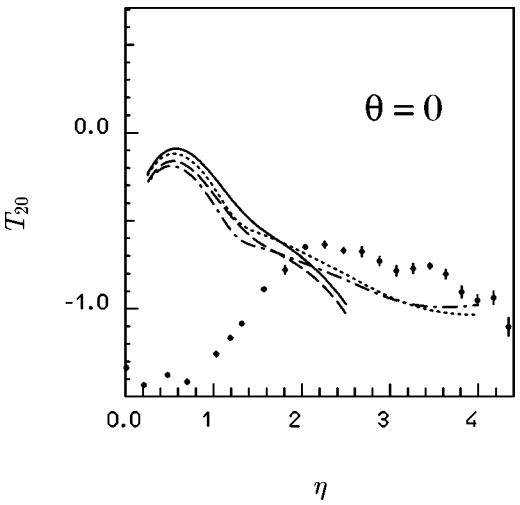

FIG. 5. Forward deuteron tensor analyzing power T_{20} using Bonn *B* (full and dotted lines) and Paris (dashed and dotted-dashed curves) potentials. For both the dotted and dotted-dashed lines the free isobar width has been employed, while the other two curves refer to the parametrization derived from πd absorption.

In Fig. 6 the results obtained for T_{20} at backward angles are compared with the experimental data. The symbolism of the figure is similar to that of the previous one. It is evident that the backward angle results are much more structured and difficult to reproduce than the forward results. Here, the data are not reproduced well in the entire energy region under consideration. The theoretical results however show a certain structured shape which is qualitatively similar to that evidenced by the data. For this observable, similarly to what was previously observed for the cross section, the backward-angle results are quite sensitive to the *NN* potential employed.

IV. SUMMARY AND CONCLUSIONS

In this paper we have carried further the analysis of the $pd \leftrightarrow \pi^+ t$ process initiated in Ref. [1] by considering the spin observables. In particular, we have studied the proton

analyzing power A_{y0} and deuteron tensor analyzing power T_{20}.

As is well known, A_{y0} is very difficult to reproduce because it depends not only on the magnitude of the various helicity amplitudes, but also on the phases of these complex quantities. We have found that the three-nucleon dynamics in the initial channel has a modest influence around the Δ resonance while in general the convergence with respect to the partial-wave representation is of great importance. In particular, orbital ΔN states greater than $L=0$ definitely have to be included. This effect on A_{y0} is somewhat different from the behavior of the unpolarized cross section, where the three-nucleon dynamics and the higher partial waves affect the results by roughly the same amount [1].

We have considered the energy dependence of T_{20} at forward and backward angles, finding that T_{20} at 0° is not very sensitive to the NN potential employed in the calculation, while the results at backward angles are much more sensitive to the nuclear potential, except for the region at threshold. This behavior of T_{20} is similar to what has been observed previously for the differential cross section. Below the resonance, the T_{20} results at forward angles are in clear disagreement with the experimental results, while above the resonance, the trend of the data is reproduced. This behavior confirms the findings already obtained from the analysis of the cross section at forward angles, and suggests that there is some missing mechanism operating at low energy. From previous experience on the $\pi d \rightarrow pp$ reaction, a very likely candidate is the process triggered by the πN s-wave interaction.

Finally, we have compared the results obtained from two different parametrizations of the Δ width. One has been obtained from the phenomenology of the $\pi d \rightarrow pp$ cross section while the other from a Chew-Low–type analysis of the πN data. While the second represents the standard parametrization of a single, free isobar, the first includes phenomenologically the interaction effects of the second nucleon on the isobar. Around the Δ resonance the differential cross section is better reproduced by the calculation with the former parametrization of the Δ width, while the latter parametrization works much better when the energy increases. This suggests that at energies above the Δ resonance the intermediate isobar propagates approximately as a free particle, while around the resonance the ΔN interaction effects are not entirely negligible.

ACKNOWLEDGMENTS

L.C. thanks B. Mayer for scientific communications. G.P. thanks the Winnipeg Institute of Theoretical Physics and University of Manitoba for support and hospitality in August and September, 1997. W.S. acknowledges financial support from INFN and from the Deutsche Forschungsgemeinschaft under Grant No. Sa 327/23-I. J.P.S. acknowledges financial support from a NATO Collaborative Research Grant (CRG. 900551), with G.P., at the very early stage of this work and the continuing financial support from NSERC, Canada. J.P.S thanks also the University of Padova and INFN for hospitality in January–April, 1995 and July, 1997.

[1] L. Canton and W. Schadow, Phys. Rev. C **56**, 1231 (1997).
[2] E. O. Alt, P. Grassberger, and W. Sandhas, Nucl. Phys. **B2**, 167 (1967).
[3] D. J. Ernst, C. M. Shakin, and R. M. Thaler, Phys. Rev. C **8**, 46 (1973); **9**, 1780 (1974).
[4] Y. Koike, J. Haidenbauer, and W. Plessas, Phys. Rev. C **41**, 396 (1987).
[5] W. Schadow and W. Sandhas, Phys. Rev. C **55**, 1074 (1997).
[6] L. Canton, J. P. Svenne, and G. Cattapan, Phys. Rev. C **48**, 1562 (1993).
[7] L. Canton, G. Cattapan, P. J. Dortmans, G. Pisent, and J. P. Svenne, Can. J. Phys. **74**, 109 (1996).
[8] P. J. Dortmans, L. Canton, and K. Amos, J. Phys. G **23**, 479 (1997).
[9] R. Machleidt, K. Holinde, and Ch. Elster, Phys. Rep. **149**, 1 (1987).
[10] M. Lacombe, B. Loiseau, J. M. Richard, R. Vinh Mau, J. Coté, P. Pirès, and R. de Tourreil, Phys. Rev. C **21**, 861 (1980).
[11] H. Garcilazo and T. Mizutani, *πNN Systems* (World Scientific, Singapore, 1990).
[12] L. Canton, A. Davini, and P. J. Dortmans, Report No. DFPD-97-TH-49, University of Padova, 1997.
[13] T. Ericson and W. Weise, *Pions and Nuclei* (Clarendon, Oxford, 1988).
[14] E. Oset, H. Toki, and W. Weise, Phys. Rep. **83**, 281 (1982).
[15] M. Jacob and G. C. Wick, Ann. Phys. (N.Y.) **7**, 404 (1959).
[16] M. Simonius, in *Polarization Nuclear Physics*, edited by D. Fick, Lecture Notes in Physics Vol. 30, (Springer-Verlag, Berlin, 1974), p. 38.
[17] J. M. Cameron, P. Kitching, J. Pasos, J. Thekkumthala, R. Abegg, D. A. Hutcheon, C. A. Miller, S. A. Elbakr, and A. H. Hussein, Nucl. Phys. **A472**, 718 (1987).
[18] G. J. Lolos *et al.*, Nucl. Phys. **A386**, 477 (1982); G. J. Lolos *et al.*, *ibid.* **A422**, 582 (1984).
[19] C. Kerboul *et al.*, Phys. Lett. B **181**, 28 (1986); B. Mayer (private communication).
[20] J. M. Laget and J. F. Lecolley, Phys. Lett. B **194**, 177 (1987).